Journal of Theoretical Biology 387 (2015) 111–119

Contents lists available at ScienceDirect

Journal of Theoretical Biology

journal homepage: www.elsevier.com/locate/yjtbi

Invasion speeds with active dispersers in highly variable landscapes: Multiple scales, homogenization, and the migration of trees

Ram C. Neupane *, James A. Powell

Department of Mathematics and Statistics, Utah State University, 3900 Old Main Hill, Logan, UT 84322-3900, USA

HIGHLIGHTS

- A new model for bird-dispersed seeds with variable handling times and habitat.
- Multi-scale, homogenized kernel reflecting large and short distance dispersal.
- A simple population model for adult plants simulates rates of invasion.
- Large scale structure of dispersal kernel provides easy invasion rate prediction.
- Harmonic average parameters predict simulated invasion speeds in variable habitat.

ARTICLE INFO

Article history:
Received 5 June 2015
Received in revised form
28 September 2015
Accepted 29 September 2015
Available online 8 October 2015

Keywords:
Homogenized dispersal kernel
Ecological diffusion
Harmonic average motility
Invasion speeds

ABSTRACT

The distribution of many tree species is strongly determined by the behavior and range of vertebrate dispersers, particularly birds. Many models for seed dispersal exist, and are built around the assumption that seeds undergo a random walk while they are being carried by vertebrates, either in the digestive tract or during the process of seed storage (caching). We use a PDF of seed handling (caching and digesting) times to model non-constant seed settling during dispersal, and model the random component of seed movement using ecological diffusion, in which animals make movement choices based purely on local habitat type instead of population gradients. Spatial variability in habitat directly affects the movement of dispersers and leads to anisotropic dispersal kernels. For birds, which can easily move many kilometers, habitat changes on the scale of tens of meters can viewed as rapidly varying. We introduce multiple scales and apply the method of homogenization to determine leading order solutions for the seed digestion kernel (SDK). Using an integrodifference equation (IDE) model for adult trees, we investigate the rate of forest migration. The existing theory for predicting spread rates in IDE does not apply when dispersal kernels are anisotropic. However, the homogenized SDK is isotropic on large scales and depends only on harmonically averaged motilities and modal rates of digestion. We show that speeds calculated using the harmonic average motility accurately predict rates of invasion for the spatially variable system.

1. Introduction

The diffusion equation represents a fundamental framework for determining the spatial spread of organisms (Hengeveld 1988; Okubo and Levin 1989; Shigesada et al., 1995; Skalski and Gilliam 2003; Morales and Carlo 2006). Fisher (1937) studied asymptotic rates of invasion of mutant genes and his ideas were extended by Skellam (1951) to ecological problems (the spread of animal and plant populations on landscape scales). Later on, diffusion equations were used to describe the spread of the cereal leaf beetle, muskrat, small cabbage white butterfly (Andow et al., 1990) and dispersal of cholla (Allen et al., 1991).

Diffusion models usually assume that animal movement properties are constant in space and time, but in fact animals move differently in different habitats. Movement occurs while animals search for food, water, breeding sites, mates and shelter. Each of these activities is conditioned by habitat type; deer do not linger to forage on barren slick rock, and birds eating juniper berries spend a great deal of time foraging on juniper trees but very little time in the sagebrush steppe separating stands of juniper. The movement properties of a population are determined by the composition of all landscape elements and the nature of the

* Corresponding author.
E-mail address: ram.neupane@aggiemail.usu.edu (R.C. Neupane).

http://dx.doi.org/10.1016/j.jtbi.2015.09.029
0022-5193/

boundaries between them (Moilanen and Hanski, 1998; Haynes and Cronin, 2003; Ovaskainen, 2004).

Spatial variation in landscape structure is one of the components that affects the mobility of active dispersers. Hanski et al. (2004) have observed that increasing environmental heterogeneity increases the variance in mobility of butterflies. Raposo et al. (2011) have shown that heterogeneous landscape enhances diffusivity and foraging behavior of dispersers under the constant density of scarce resources. Habitat fragmentation is a special kind of variability; Dewhirst and Lutcher (2009) have demonstrated that spread rate of populations increases in fragmented habitat in the absence of Allee effect (but decreases when there is an Allee effect).

At population and landscape scales movement is often modeled by Fickian diffusion (Reeve et al., 2008), in which population redistribution is driven by population gradients. This means that the movement of individuals tends from higher concentrations to lower concentrations, and changes in local habitat only alter the movement rate down the gradient (Okubo and Levin, 2001). However, animal responses to spatial heterogeneity are not likely to be Fickian. When deer bed down at or inside a treeline they do not randomly diffuse past the forest edge, and when American robins forage for juniper berries they exhibit high fidelity to the location of the trees and simply avoid the surrounding steppe, unless they are choosing to move between patches of juniper. In both of these cases the animals are making movement choices based on the patch of habitat in which they currently reside, not perceptions of population gradients. A more appropriate way to describe animal movement in which organisms make random steps based on current habitat types is “ecological diffusion” (Turchin, 1998). In this approach differences in population dispersion are driven by residence times in differing habitat types. Where residence times are high (in juniper for robins) populations accumulate, and where residence times are low (in sagebrush) the population density is low. An ecological diffusion model supports discontinuous solutions at boundaries, consequently, deer can accumulate inside of a forest patch without diffusing out into the adjacent meadow against their will. Turchin (1998) observed that residence time and motility (the analog of diffusivity) are inversely proportional. Thus, if the motility is low in a patch (residence time is high) then individuals do not choose to leave the patch very frequently and the population density increases.

Seed transport during vertebrate movement happens mainly in two ways. Dispersal agents either hide seeds at some distance from the fruiting tree for future use or these agents eat seeds and defecate seeds at some new location. When animal motility is independent in space, Neubert et al. (1995) have discussed two limiting cases of seed spread. If every dispersal agent requires exactly the same amount of time to handle individual seeds, seed dispersal on the landscape is Gaussian. On the other hand, if these agents drop seeds at a constant rate in both time and space, seed spread in a Laplace distribution. Both extremes, however, are unlikely in real life scenarios. Neupane and Powell (2015) hypothesized that handling time is sampled from a distribution after seeds are picked. Using a time-dependent seed handling function they calculated seed digestion kernels (SDK). Neupane and Powell showed that the SDK accurately described seed dispersal for pinyon pine and Utah juniper, as reflected in the historical migration rate of these species.

Dispersal kernels in spatially variable landscapes have not received much attention. Simple analytic solutions do not exist for arbitrarily structured spatial landscapes. Numerical approaches are possible, but would require the user to solve the diffusion/settling equations separately for each generation with different initial conditions for each generations' new location of seed sources. The computational cost of this operation would increase geometrically with landscape complexity. If spatial discretization is chosen small enough to resolve the smallest landscape features, a general rule to maintain numerical stability is that time steps must scale with the square of the size of spatial discretization ($\Delta t \leq C\Delta x^2$, Ascher and Greif 2011). Thus the number of computations tends to follow the cube of the spatial discretization, becoming unattractive for large, complex landscapes.

However, if the scale of spatial variability is very short as compared with the movement capacity of individuals, as occurs with vertebrate dispersers of tree seeds and berries, it is possible to solve Neubert's system analytically using the method of homogenization (Powell and Zimmermann 2004; Garlick et al. 2010). In this multi-scale procedure, slow and fast dispersal scales are introduced, linked by an asymptotically small order parameter. Solutions are then described by a regular perturbation series, leading to a large-scale solvability condition (the “homogenized equation”) which determines large-scale solution behavior (Holmes 1995). Powell and Zimmermann (2004) used the homogenization technique to analyze active seed dispersal and forest migration in a heterogeneous landscape, but these authors were working in a Fickian diffusion framework and used constant settling rates instead of sampling the variability in seed handling times. On the other hand, Garlick et al., (2013) used homogenization in an ecological diffusion model to investigate the spread of chronic wasting disease in mule deer, but again the contact rates were assumed to be constant instead of modal.

Musgrave and Lutcher (2014a) constructed diffusion model for random walk assuming that diffusion, settling and mortality rates are discontinuous step functions depending on the structure of habitat patches in the landscape. The model was used to derive dispersal kernels, investigate critical patch sizes for population growth and examine invasions. They hypothesized that dispersal distance is smaller than the size of habitat patch. Initially they chose a bounded habitat patch to estimate kernels. They further explored the kernels in the periodic heterogeneous landscape for the different quality of habitat patches. Musgrave and Lutcher (2014b) also extended their work to find invasion speeds using estimated kernels associated with individual movement behavior. Robbins (2004) discussed very similar mechanistic models for seed dispersal in a two patch, periodic setting. In both Robbins (2004) and Musgrave and Lutscher (2014a, 2014b), due to the simple periodicity of the patch structure and assumption of piecewise constant parameters the authors were able to avoid multiscale analysis in favor of exact, analytic procedures. On the other hand, time-dependent rates of settling, necessary to understand seed caching and rates of seed digestion, were not considered, and the patches considered were of only two types (“good” and “bad”), and the landscape comprised of periodic repetition of these two patches.

In this paper we adapt a dispersal model from Neubert et al. (1995) by introducing ecological diffusion with highly variable motility and a modal distribution of seed handling times. We assume that motility varies on short scales and use multiple scales in space and time to apply the method of homogenization for solving the model. Using a solvability condition, we derive a simple constant diffusion equation on large scales and approximate the SDK. This kernel depends on the harmonic average of the motility. We then embed the kernel into an integrodifference equation (IDE) population model for adult plants. The large scale diffusion equation depends on small-scale variability only through the harmonically averaged motility, which inflicts a large-scale isotropic structure on the dispersal kernel. We hypothesize that the harmonic average motility therefore predicts the invasion speed in spatially complex environments. Analytic and numerical simulation methods are used to compare predicted and observed migration speeds. We conclude that observed speed converges asymptotically to the predicted constant speed.

2. Methods

2.1. Dispersal model on a variable landscape

We introduce a modified version of the Neubert et al. (1995) seed dispersal model to accommodate ecological diffusion and a distribution of seed handling times for vertebrate dispersers of tree seeds. We assume that motility depends only on space, while the distribution of seed handling times depends only on time (that is, time required for digestion is intrinsic to the dispersers, not the habitat). Thus

$$\partial_t(P) = \partial_x^2(D(x)P) - h(t)P, \quad P(x, t=0) = \delta(x-x'), \tag{1}$$

$$\partial_t(S) = h(t)P, \qquad S(x, t=0) = 0, \tag{2}$$

where $P(x,t)$ represents the density of seeds during dispersal by frugivorous birds and animals moving in the variable landscape, $D(x)$ is the seed motility rate while being carried by dispersers and $h(t)$ is the hazard function or rate of seed settling. To model real-world variability in the amount of time that seeds spend being carried by dispersers (i.e. distribution of times at which seeds are digested and defecated or carried and cached) we take $h(t)$ to be a probability density function (PDF) in time (Neupane and Powell, 2015). Finally, $S(x,t)$ is the seed density on the landscape at time t. The Dirac delta function, $\delta(x-x')$, gives initial seed position at x' and $S(x, t=0) = 0$ because there are no seeds dispersed at time $t=0$. The long-time limit of this process will generate a seed digestion kernel (SDK), which is the probability of a seed moving from the starting location, x', to a final location on the landscape, x.

The term $(D(x)P)_{xx}$ was used by Turchin (1998) to describe "ecological diffusion" for bird or animal movement decisions based purely on local habitat properties. Unlike standard, Fickian diffusion, in which populations disperse along gradients and eventually become constant, but at rates proportional to the diffusion rate, in ecological diffusion the residence time of individuals is inversely proportional to the "motility", $D(x)$. Consequently the long-term results of movement choices are that populations tend to aggregate where residence times are high (low motility) and avoid locations with high motility (low residence time). We restrict ourselves to one dimension and assume $P, S \to 0$ as $|x| \to \infty$ to analyze rates of spread perpendicular to a wave of invasion.

Following Neupane and Powell (2015), we assume that the PDF of seed handling times (digestion or caching) by birds and animals is represented by the distribution

$$h(t) = \frac{a\, t^{\alpha}}{b^{\beta} + t^{\beta}}, \quad \beta > \alpha + 1 > 0. \tag{3}$$

Here b scales the mean seed handling time and a is a normalization constant. Notice that $h(t) \sim t^{\alpha}$ as $t \longrightarrow 0$ while $h(t) \sim t^{\alpha-\beta}$ as $t \longrightarrow \infty$.

To find the seed distribution on the landscape associated with the hazard function defined in Eq. (3), we need to solve the model (1) and (2). First, define $f(t)$ as

$$f(t) = \int_0^t \frac{a\tau^{\alpha}}{b^{\beta} + \tau^{\beta}} d\tau, \tag{4}$$

so $f'(t) = h(t)$. Then, Eq. (1) becomes

$$\partial_t(P) = \partial_x^2(DP) - f'(t)P. \tag{5}$$

Multiplying on both sides of the equation by the integrating factor, $e^{f(t)}$, and rearranging terms, we arrive at the equation

$$\frac{\partial}{\partial t}\left(Pe^{f(t)}\right) = \partial_x^2(DPe^{f(t)}). \tag{6}$$

If

$$u = Pe^{f(t)} \tag{7}$$

Eq. (6) becomes

$$\partial_t(u) = \partial_x^2(D(x)u). \tag{8}$$

2.2. Introduction of multiple scales for highly variable landscapes

We introduce multiple scales to model highly variable habitat motility in Eq. (8). Let y, the small scale, be $y = \frac{x-x'}{\varepsilon}$ for some order parameter $0 < \varepsilon \ll 1$. The order parameter captures the difference in scale between the patchiness of the landscape and the larger scale at which vertebrate dispersers can move. For example, landcover mapping via geographic information systems is generally framed on 30 m pixels because habitat varies on scales of tens of meters. On the other hand, birds typically fly distances which are measured in terms of kilometers, so we would take $\varepsilon = \frac{10\text{ m}}{1\text{ km}} = 0.01$. We assume motility varies on both scales, so that $D = D(x, y = \frac{x-x'}{\varepsilon})$. In the context of ecological diffusion, D reflects movement choices being made because of current habitat type. Thus, the multi-scale assumption means that habitat is varying on short scales (i.e. patches of trees and meadows varying over tens of meters) as well as large scales (i.e. the relative spacing of patches and meadows varies over kilometers due to elevation, soil type, exposure). Validation of these assumptions on real landscapes is presented by Garlick et al. (2010). With the new scales, spatial derivatives are rewritten as

$$\partial_x \longrightarrow \frac{1}{\varepsilon}\partial_y + \partial_x,$$

$$\partial_x^2 \longrightarrow \frac{1}{\varepsilon^2}\partial_y^2 + \frac{1}{\varepsilon}2\partial_x\partial_y + \partial_x^2.$$

We must also choose a fast time scale to balance the short space scale. Taking $\tau = \frac{t}{\varepsilon^2}$. the time derivative transforms into

$$\partial_t \longrightarrow \frac{1}{\varepsilon^2}\partial_\tau + \partial_t.$$

Applying these transformations to Eq. (8) gives

$$\left(\frac{1}{\varepsilon^2}\partial_\tau + \partial_t\right)u = \left(\frac{1}{\varepsilon}\partial_y + \partial_x\right)^2 [D(x,y)u]. \tag{9}$$

Assume that the solution can be expanded as a regular asymptotic series,

$$u = u_0 + \varepsilon u_1 + \varepsilon^2 u_2 + O(\varepsilon^3). \tag{10}$$

Multiplying by ε^2, Eq. (9) becomes

$$(\partial_\tau + \epsilon^2\partial_t)(u_0 + \epsilon u_1 + \ldots) = \left(\partial_y + \epsilon\partial_x\right)^2 [D(x,y)(u_0 + \epsilon u_1 + \ldots)],$$

which can be expanded

$$\partial_\tau u_0 + \varepsilon\partial_\tau u_1 + \varepsilon^2[\partial_t u_0 + \partial_\tau u_2] + \ldots = \partial_y^2(Du_0) + \varepsilon\left[\partial_y^2(Du_1) + 2\partial_x\partial_y(Du_0)\right] + \varepsilon^2[\partial_y^2(Du_2) + 2\partial_x\partial_y(Du_1) + \partial_x^2(Du_0)] + \ldots. \tag{11}$$

2.3. Homogenization technique applied to rescaled seed dispersal model

2.3.1 Solution at $\boldsymbol{O}(1)$

The method of homogenization is essentially to solve the multi-scale expansion (11) at successive orders of ε, being alert for a solvability condition which will reconcile the solution across scales. Equating terms at leading order in (11) gives

$$\partial_\tau u_0 = \partial_y^2(D(x,y)u_0). \tag{12}$$

This is a parabolic equation and its solution relaxes exponentially to the steady state on the fast time scale. Since we are seeking the long-time limit of the process, we can ignore

transients, giving

$$\partial_y^2(D(x,y)u_0)=0. \tag{13}$$

The solution of this equation is

$$u_0=\frac{C_0(x,t)}{D(x,y)}+\frac{C_1(x,t)}{D(x,y)}y.$$

Recall that the small scale and dispersal are related as $y=\frac{x-x'}{\varepsilon}$. In order to have bounded solutions as $\varepsilon\to 0$ that is, $|y|\to\infty$),we require

$$u_0=\frac{C_0(x,t)}{D(x,y)}. \tag{14}$$

2.3.2 Solution at $\boldsymbol{O(\varepsilon)}$

Equating the terms at order ε from the expanded form of Eq. (11) gives

$$\partial_\tau u_1=\partial_y^2(D(x,y)u_1)+2\partial_x\partial_y(Du_0). \tag{15}$$

Using u_0 from (14) gives $2\partial_x\partial_y(Du_0)=2\partial_x\partial_y(c_0(x,t))=0$. Then Eq. (15) gives

$$\partial_\tau u_1=\partial_y^2(D(x,y)u_1).$$

This is again parabolic with exponentially decaying transients on fast time scales. Thus, $\partial_y^2(D(x,y)u_1)=0$,

which has solution

$$u_1=\frac{d_1(x,t)}{D(x,y)}+\frac{d_2(x,t)}{D(x,y)}y.$$

Once again, for the solution to be bounded as $\varepsilon\longrightarrow 0$,

$$u_1=\frac{d_1(x,t)}{D(x,y)}. \tag{16}$$

2.3.3. Solvability condition at $\boldsymbol{O(\varepsilon^2)}$

Equating terms with ε^2 from the expanded form of Eq. (11) gives

$$\partial_\tau u_2+\partial_t u_0=\partial_y^2(Du_2)+\partial_x^2(Du_0)+2\partial_x\partial_y(Du_1). \tag{17}$$

From Eq. (16), $\partial_x\partial_y(Du_1)=\partial_x\partial_y(d_1(x,t))=0$,and using the fact that $\partial_\tau u_2\to 0$ in long time, Eq. (17) gives

$$\partial_t\left(\frac{C_0}{D}\right)=\partial_y^2(Du_2)+\partial_x^2(c_0). \tag{18}$$

Rearranging terms in Eq. (18) gives

$$\partial_y^2(Du_2)=\partial_x^2(c_0)-\partial_t\left(\frac{C_0}{D}\right).$$

Integrating this equation with respect to y from $-l$ to l,

$$\partial_y(Du_2)|_{y=-l}^{y=l}=\partial_x^2(c_0)\int_{-l}^{l}dy-\partial_t(c_0)\int_{-l}^{l}\frac{1}{D}dy. \tag{19}$$

As Holmes (1995) points out, the right hand side of this equation grows in proportion to l for arbitrary c_0 and bounded, nonzero motility. However, the left hand side is bounded and remains small. Thus, Eq. (18) becomes unsolvable unless there is something special about c_0. To continue the perturbation approach and generate a bounded solution for u_2, the right hand side must be zero as $l\to\infty$; thus we have a stability condition as $l\longrightarrow\infty$,

$$2l\partial_x^2(c_0)-\partial_t(c_0)\int_{-l}^{l}\frac{1}{D}dy=0. \tag{20}$$

Define the average of a function w as

$$\langle w\rangle=\lim_{l\to\infty}\frac{1}{2l}\int_{-l}^{l}w(y)dy.$$

The second term in the solvability condition can be written

$$\left\langle\partial_t\left(\frac{c_0}{D}\right)\right\rangle=\left\langle D^{-1}\right\rangle\partial_t c_0, \tag{21}$$

where $\overline{D}=\frac{1}{\langle D^{-1}\rangle}$, the harmonic average of D and $\langle D^{-1}\rangle$ gives the average of D^{-1}.

From Eqs. (18), (20) and (21) we now have

$$\partial_t c_0=\overline{D}(x)\partial_x^2 c_0;\quad c_0(x,x',0)=D(x',0)\,\delta(x-x'), \tag{22}$$

where $D(x',0)$ is the motility at the seeds' starting location, x'.

2.4. Solving for seed dispersal

We assume $\overline{D}$ is locally constant, so that the solution to (22) can be written

$$c_0(x,x',t)=\frac{D(x',0)}{\sqrt{4\pi\overline{D}\,t}}e^{\frac{-(x-x')^2}{4\overline{D}t}}. \tag{23}$$

From Eqs. (10) and (14) we have

$$u(x,y,t)=\frac{c_0(x,t)}{D(x,y)}+O(\varepsilon). \tag{24}$$

Returning to the original dependent variable, Eqs. (7), (23) and (24) give

$$P(x,x',y,t)\cong\frac{c_0(x,t)}{D(x,y)}e^{-f(t)}=\frac{D(x',0)}{D(x,y)\sqrt{4\pi\overline{D}t}}e^{-f(t)}e^{\frac{-(x-x')^2}{4\overline{D}t}}, \tag{25}$$

and returning to unscaled spatial variables we have

$$P(x,x',t)\cong\frac{c_0(x,t)}{D(x)}e^{-f(t)}=\frac{D(x')}{D(x)\sqrt{4\pi\overline{D}t}}e^{-f(t)}e^{\frac{-(x-x')^2}{4\overline{D}t}}, \tag{26}$$

where $D(x)=D(x,0)$ and $D(x')=D(x',0)$.

Integrating Eq. (2) using (26),

$$\begin{aligned}S(x,x',t)&\cong\frac{D(x')}{D(x)}\int_0^t\left(\frac{h(t')}{\sqrt{4\pi\overline{D}t'}}e^{-f(t')}e^{\frac{-(x-x')^2}{4\overline{D}t'}}\right)dt'\\&=\frac{D(x')}{D(x)}\int_0^t\left(\frac{h(t')}{\sqrt{4\pi\overline{D}t'}}e^{-\int_0^{t'}h(\tau)d\tau}e^{\frac{-(x-x')^2}{4\overline{D}t'}}\right)dt'.\end{aligned} \tag{27}$$

2.5. Homogenized seed dispersal kernel

Eq. (27) is the homogenized solution of (2) in the long time scale t and the seed digestion kernel is the long time limit of this solution. Thus the homogenized seed digestion kernel (HSDK) becomes

$$K(x,x')\cong\lim_{t\to\infty}S(x,x',t)=\frac{D(x')}{D(x)}\int_0^\infty\left(\frac{h(t)}{\sqrt{4\pi\overline{D}t}}e^{-\int_0^t h(\tau)d\tau}e^{\frac{-(x-x')^2}{4\overline{D}t}}\right)dt. \tag{28}$$

The terms $D(x)$ and $D(x')$ denote dispersal motilities at the starting and ending locations, respectively. Note that, while the homogenization approach has made the form of this solution fairly simple, it is not guaranteed to be a PDF in space; normalization is necessary before (28) can be used for seed dispersal (as we will discuss below). Consider the effect of the quotient $\frac{D(x')}{D(x)}$ on the shape of the kernel. If $D(x')$ is high, the quotient $\frac{D(x')}{D(x)}$ is relatively large and more seeds will disperse from the starting location. On the other hand, at some target location, x, if $D(x)$ is large then residence times are very small at x; the quotient is correspondingly small and it is difficult for seeds to end up near x. The shape of dispersal kernel with variable motility is shown in Fig. 1. Now we consider two limiting cases which generate closed form HSDK.

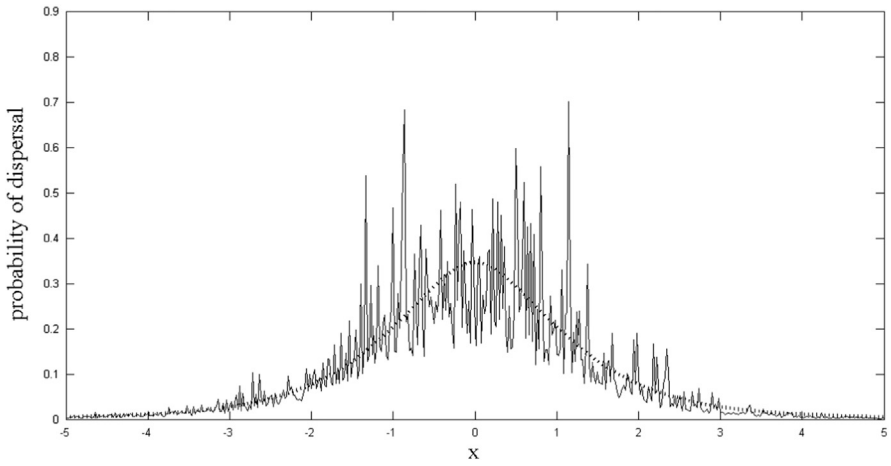

Fig. 1. This plot gives the shape of seed digestion kernel (dotted line) with constant motility $\overline{D}$ versus the homogenized seed digestion kernel (solid) with variable motility. The jaggedness of the homogenized curve is generated by random variations in motility, $D(x)$, on short spatial scales. We have chosen D from a uniform distribution between $D_{min}=.01$ and $D_{max}=.04$,assumed to be constant for each grid cell (of size $\Delta x=0.2$). We further have chosen the mean handling time $\tilde{b}=7$ and the dispersal starting location $x'=0$.

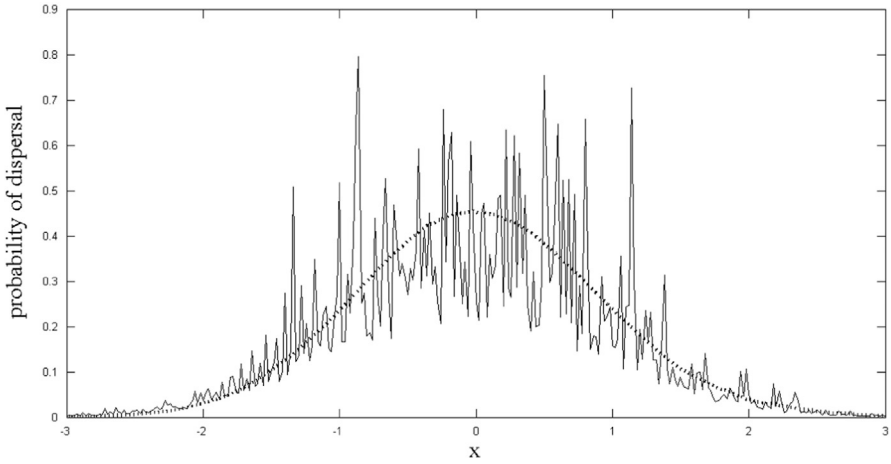

Fig. 2. This graph shows the Gaussian kernel (dotted line) with constant motility $\overline{D}$ vs the homogenized Gaussian kernel (solid) with variable motility. The jaggedness of the homogenized curve is generated from the smooth Gaussian by random variations in motility, $D(x)$, on short spatial scales. We have chosen D from an uniform distribution between $D_{min}=.01$ and $D_{max}=.04$, assumed to be constant for each grid cell (of size $\Delta x=0.2$). We also have chosen the mean handling time $\tilde{b}=7$ and the dispersal starting location is $x'=0$.

2.6. Homogenized Gaussian dispersal kernel

Based on Neupane and Powell (2015), when there is no variability in handling times, the function $h(t)$ becomes

$$h(t)=\delta\left(t-\tilde{b}\right), \tag{29}$$

where $\tilde{b}$ was defined as the maximum time spent by frugivorous birds for seed caching or seed digestion.

Then (28) can be integrated directly,

$$G(x,x')=\frac{D(x')}{D(x)}\int_0^{\infty}\left(\frac{\delta(t-\tilde{b})}{\sqrt{4\pi\overline{D}t}}e^{-\int_0^t\delta(\tau-\tilde{b})d\tau}e^{\frac{-(x-x')^2}{4\overline{D}t}}\right)dt=\frac{D(x')}{D(x)\sqrt{4\pi\overline{D}\tilde{b}}}e^{\frac{-(x-x')^2}{4\overline{D}\tilde{b}}}. \tag{30}$$

This is a homogenized version of the Gaussian kernel, depicted in Fig. 2. Note that the skeleton of the HDSK is a normal PDF in space with $\sigma^2=2\overline{D}\tilde{b}$, modulated up and down by the relative motilities at the starting and ending locations. If motility is constant, $G(x, x')$ reduces to the standard Gaussian SDK.

2.7. Homogenized Laplace dispersal kernel

Another analytic limit comes from taking the PDF h to be a step function,

$$h(t)=\begin{cases}\frac{1}{2\tilde{b}}, & 0<t\le 2\tilde{b},\\ 0, & t>2\tilde{b}.\end{cases} \tag{31}$$

where $\tilde{b}$ is the mean handling time; the hazard function is written this way to facilitate comparison with the more general SDK. It was shown in Neupane and Powell (2015) that the solution to model (1) and (2) with the step function (31) can be approximated by

$$\partial_t(P)=\partial_x^2(D(x)P)-\frac{1}{2\tilde{b}}P \quad P(x,t=0)=\delta(x-x'), \tag{32}$$

$$\partial_t(S)=\frac{1}{2\tilde{b}}P \qquad S(x,t=0)=0. \tag{33}$$

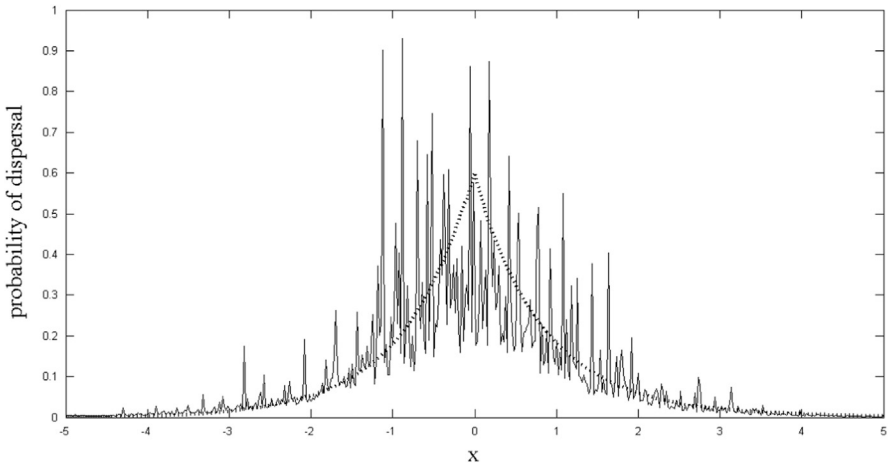

Fig. 3. This graph shows the Laplace kernel (dotted line) with constant motility $\overline{D}$ vs the homogenized Laplace kernel (solid) with variable motility. The jaggedness of the homogenized curve is generated from the smooth Laplace kernel by random variations in motility, $D(x)$, on short spatial scales. We have chosen D from an uniform distribution between $D_{min}=.01$ and $D_{max}=.04$, assumed to be constant for each grid cell (of size $\Delta x=0.2$). We also have chosen mean handling time $\tilde{b}=7$ and the dispersal starting location is $x'=0$.

Replacing h with the constant $\frac{1}{2\tilde{b}}$ in (28),

$$L(x,x')=\frac{D(x')}{D(x)}\int_0^\infty\left(\frac{\frac{1}{2\tilde{b}}}{\sqrt{4\pi\overline{D}t}}e^{-\frac{t}{2\tilde{b}}}e^{\frac{-|x-x'|}{4\overline{D}t}}\right)dt.$$

This latter integral can be evaluated (Neupane and Powell, 2015) to give

$$L(x,x')=\frac{D(x')}{D(x)2\sqrt{2-D\tilde{b}}}e^{\frac{-|x-x'|}{\sqrt{2\overline{D}\tilde{b}}}}. \tag{34}$$

This is a homogenized Laplace kernel, depicted in Fig. 3. Note that the skeleton of this distribution is a Laplace PDF in space with mean dispersal distance $\sqrt{-D\tilde{b}}$, modulated up and down by the relative motility at starting and ending locations.

2.8. A population model for adult plants

We would like to understand how spatial variability affects the effective migration rates of plants, based on the seed distribution we estimated in Eq. (28). We introduce a simple population model which includes spatially varying dispersal,

$$N_{n+1}=\underbrace{T\left[K(x,x')^{*}kN_n(x)\right]}_{\text{Newly dispersed survived seeds to germinate}}+\underbrace{(1-\omega)N_n(x)}_{\text{Survived old adults}} \tag{35}$$

where N_n is the population density of adults in generation n, $K(x,x')$ gives the dispersal kernel, k is the number of seeds produced per adult per generation, ω gives the mortality probability of adults per generation, and

$$T=\frac{Mg\sigma N_n}{M+N_n}$$

is the Beverton–Holt model for the number of seedlings surviving in competition with other seedlings after germination. In this model, g is the germination rate, σ is the seed survival rate and M is the maximum density of surviving seeds. The convolution in (35) is defined by

$$K(x)*kN_n(x)=\int_{-\infty}^{\infty}K(x,x')\,k\,N_n(x')dx'. \tag{36}$$

Notice that the dispersal kernel derived in Eq. (28) is anisotropic. Consequently the integrodifference Eq. (35) can not be evaluated rapidly from generation to generation using Fast Fourier Transforms; as it stands the convolution must be evaluated numerically at every location using direct quadrature.

2.9. Invasion speed estimation

We use the population model (35) to estimate the speed of invasion in a variable landscape. Since the dispersal kernel is anisotropic we cannot evaluate invasion speeds directly by following the method of Kot et al. (1996). However, the homogenized solutions have large scale structure which is isotropic, with spatial parameters determined by the harmonic average ($\overline{D}$) of D. We therefore hypothesize that the speeds can be predicted using the isotropic kernel and the harmonic average motility. That is, for purposes of predicting speeds we will use the isotropic dispersal kernel, $\overline{K}(x-x')$ which provides the skeleton of the HDSK:

$$K(x,x')=\frac{D(x')}{D(x)}\overline{K}(x-x')=\frac{D(x')}{D(x)}\int_0^\infty\left(\frac{h(t)}{\sqrt{4\pi\overline{D}t}}e^{-\int_0^t h(\tau)d\tau}e^{\frac{-(x-x')^2}{4\overline{D}t}}\right)dt.$$

Here $\tilde{b}$ is the mode of $h(t)$, which we use to facilitate comparison among the various kernels (see Neupane and Powell (2015) for details).

We outline the method of Kot et al. (1996). Far in advance of the wave of invasion we assume that population density approaches zero as $x\to\infty$,

$$N_n(x)\sim\varepsilon e^{-ux}, \tag{37}$$

with $\varepsilon\ll 1$ (note this is not the ε from homogenization). At a constant speed of invasion, c, the spreading population can be written as

$$N_{n+1}(x)=N_n(x-c). \tag{38}$$

Eqs. (37) and (38) give

$$N_{n+1}(x)=\varepsilon e^{-u(x-c)}. \tag{39}$$

Putting this all into Eq. (34),

$$\varepsilon e^{-u(x-c)}\sim T\left[-K(x-x')*\varepsilon\,k\,e^{-ux}\right]+\varepsilon(1-\omega)\,e^{-ux}. \tag{40}$$

Applying a Taylor expansion for $T(\bullet)$ (and observing $T(0)=0$),

$$e^{-u(x-c)}\sim kT'(0)-K(x-x')*e^{-ux}+(1-\omega)e^{-ux}+O(\varepsilon). \tag{41}$$

Equating leading order terms of Eq. (41) gives

$$e^{-u(x-c)}=R_0-K(x-x')*e^{-ux}+(1-\omega)e^{-ux}, \tag{42}$$

where $R_0=kT'(0)=kg\sigma$ is the net reproductive rate.

The moment generating function, M, of the skeletal dispersal kernel is defined as

$$M(u) = \int_{-\infty}^{\infty} -K(v)e^{-uv}dv \tag{43}$$

and thus we arrive at a dispersion relation relating c and u,

$$e^{cu} = R_0M(u)+(1-\omega), \tag{44}$$

from which

$$c = \frac{R_0M'(u)}{R_0M(u)+(1-\omega)}. \tag{45}$$

Using (44) to eliminate c we get a single equation whose roots determine u,

$$F(u) = u\frac{R_0M'(u)}{R_0M(u)+(1-\omega)} - \log\left[R_0M(u)+(1-\omega)\right] = 0. \tag{46}$$

The moment generating function and its derivative can be calculated numerically using the trapezoid rule; roots of F are found numerically using fzero in MATLAB. The numerical roots then generate the speed of invasion from Eq. (45).

3. Results

For constant motility Neupane and Powell (2015) have already calculated invasion speeds for the Beverton–Holt population model. Speeds of the SDK fall between speeds generated by the Gaussian and Laplace dispersal kernels for large $\tilde{b}$ while for smaller $\tilde{b}$ the fact that $h(t)$ is not compactly supported make the speeds of SDK invasions higher than either Gaussian or Laplace invasions. Here we test whether the speeds predicted using the skeletal kernel, $\overline{K}$, and harmonic motility, $\overline{D}$, accurately predict speeds resulting from simulated invasions with highly variable motility $D(x)$.

3.1. Simulating invasions using the homogenized population model

3.1.1. Evaluating HSDK numerically

To resolve HSDK numerically, we calculate the integral (28) using the trapezoid rule in x at every starting location x' and save these values, giving the kernel at different locations. The kernels calculated in this way are accurate to $O(\varepsilon \approx .01)$ but may not be PDFs because the homogenization procedure does not necessarily preserve the norm. We therefore normalize the kernels numerically. Boundaries must be carefully handled in this calculation. The mean variance of seeds during dispersal is $\sigma = \sqrt{2\overline{D}\tilde{b}}$. For a Gaussian distribution this means that 99.7% of dispersed seeds fall within 3σ of their starting location (Casella and Berger, 2001). Outside this boundary seed dispersal is negligible. For a simulation domain $x \in (-L, L)$ we choose $(-L+3\sigma, L-3\sigma)$ as our computational domain. This creates two buffer zones on either end of the simulation domain. Seeds may disperse into the buffer zone, but seeds are not allowed to disperse out of the buffer zone. Thus dispersal kernels need not be calculated inside the buffer zones, where they can not be normalized. The harmonic average motility,

$$\overline{D} = \frac{1}{2l}\int_{x'-l}^{x'+l} \frac{1}{D(y)}dy,$$

is calculated numerically using the trapezoid rule with $l = \min(3\sigma, 10)$.

3.1.2. Numerical simulation and invasion speed diagnosis

To estimate invasion speed, we run the simulation for 20 generations and then identify the isocline $N_n = 1$, where N_n is the population after n generations (see Fig. 4, top). In each generation we measure the farthest forward distance along the isocline. The last ten of these distances is fit to a line using regression; the diagnosed wave speed, c_{obs}, is the slope of this line (Fig. 4, bottom).

3.2. Speed comparison

We have chosen $D = .01 + .02 * \left[\left\{\frac{1+\cos\left(\frac{2\pi x}{2}\right)}{8}\right\}\right]^2$ in the simulation so that all simulations have the same motility structure regardless of discretization. For $\tilde{b}$ between 1 and 20 we compare observed speeds computed using the HSDK in (35) with predicted speeds using the harmonic average motility, $\overline{D}$. As might be expected on dimensional grounds, the predicted speed scales with $\sqrt{\overline{D}\tilde{b}}$. However, in spite of the high variability of $D(x)$, observed invasion speeds conform closely to the predictions using homogenized motility (see Fig. 5).

While predicted and observed speeds are close, they are not precisely the same. There are two sources of error, one in diagnosing the observed speeds using linear regression (which should be of size $\Delta x = 0.1$ and unbiased) and the other due to convergence in time. Based on Kot and Neubert (2008), observed

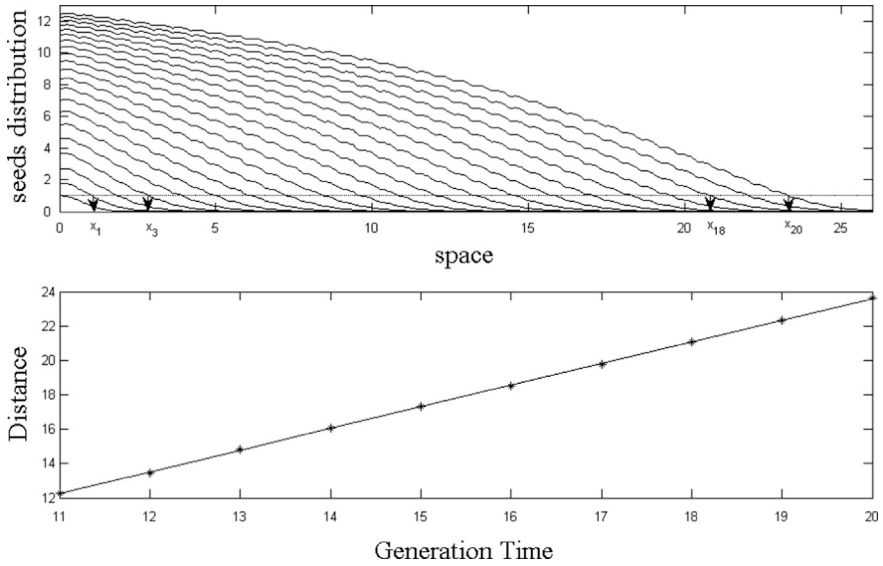

Fig. 4. The top figure shows the invasion front wave simulated up to 20 generations. The dotted isocline meets with each wave giving a corresponding distance in space. In the bottom figure the last ten distances are fit to a line; the slope of this line gives the observed speed of invasion.

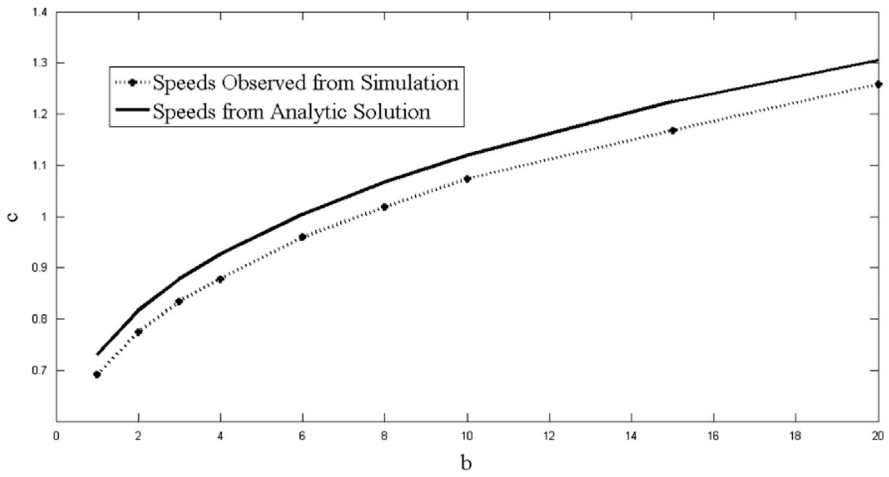

Fig. 5. The solid line gives the speeds with seed digestion kernel. This kernel is estimated analytically from dispersal model for constant motility rate. The dotted line indicates the speeds with the kernel from numerical simulation using the harmonic average of variable motility rate. The graph shows that both speeds are closely increasing in the same pattern as mean digestion time scaling parameter b increases.

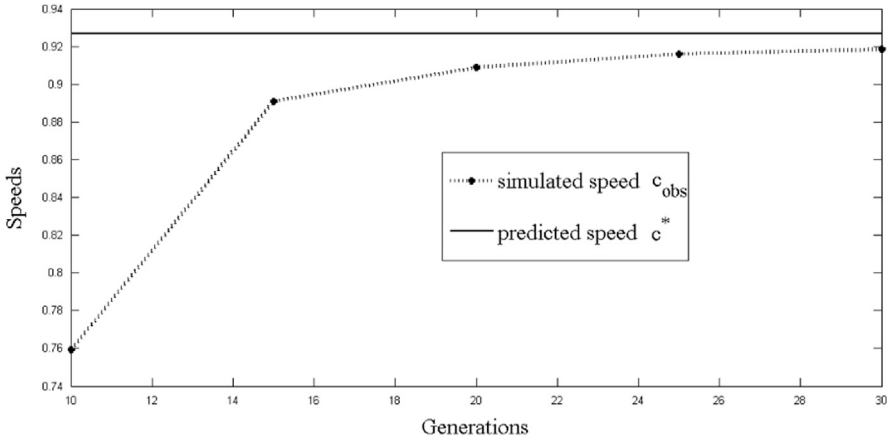

Fig. 6. The solid (-) horizontal line represents the invasion speed predicted (c^*) from the analytic solution of dispersal model. The dotted line (…) gives the speed estimated (c_{obs}) from numerical simulation. As the number of generations increases, the simulated speed approaches the predicted speed at a rate like $1/n$, per Kot and Nuebert (2008).

speeds should converge from below at a rate like $\frac{1}{n}\log\sqrt{2\pi n c_1}$ (with c_1 a constant, see Kot and Neubert (2008) Eq. (52)). To test that observed speeds are actually converging to predicted speeds we performed a convergence study at $\tilde{b}=4$, running the same simulation for between 10 and 30 generations (results depicted in Fig. 6). Results indicate that the observed invasion speeds are converging to predicted speeds as expected.

4. Conclusion

Landscape variability is one of the factors that directly affects the motility of dispersers. Consequently, seed dispersal by active dispersers varies considerably with habitat structure within the landscape. In this paper we have adapted an existing model for active seed dispersal to highly variable landscapes, introducing ecological diffusion (so that disperser motility depends on habitat type alone) and modal seed handling times. We introduce multiple scales to resolve the effect of rapidly varying habitats and solve the dispersal model using the method of homogenization. The resulting homogenized seed digestion kernel has asymptotically correct large scale isotropic structure conditioned by the harmonic average motility ($\overline{D}$) and appropriate anisotropic small scale variation for seed dispersal reflecting highly variable habitat. This represents a significant advance. Using the formulae derived here analytic predictions for seed dispersal can be generated for arbitrary (but highly variable) landscapes; previously the only available methods would have been tedious and unwieldy numerical computations.

We have also used the homogenized dispersal kernels to calculate rates of invasion in variable landscapes. Using a simple integrodifference equation for adult plants, we include the effects of spatial variability via convolution of the anisotropic dispersal kernels. No general results exist for predicting *a priori* spread rates of adult plants in such circumstances. However, we observe that the homogenized kernels have isotropic large-scale structure, conditioned on the small scale only through the harmonically averaged motility. Using existing theory for predicting spread rates for isotropic dispersal kernels we predict rates of invasion in the IDE model using $\overline{D}$ and compare with simulated invasions for the IDE and spatially complicated dispersal. Our results show that the *a priori* predictions using $\overline{D}$ accurately predict observed invasions, and a convergence study shows that the simulated fronts converge inversely with the number of generations, as predicted by the isotropic theory. This represents a second novel contribution; rates of invasion can now be predicted in arbitrary, rapidly-varying environments.

Acknowledgments

The authors would like to thank Luis Gordillo, Jacob Duncan and USU's MathBio group for giving RCN much helpful feedback. Authors would also like to thank to Thomas Robbins for providing a copy of his

dissertation. RCN was fully supported by a grant from USU's Research of Graduate Studies. JAP would also like to thank the NSF for support under DEB Grant 0918756 as well as the Western Wildland Environmental Threat Assessment Center (WWETAC).

References

Allen, L.J.S., Allen, E.J., Kunst, C.R.G., Sosebee, R.E., 1991. A diffusion model for dispersal of Opuntia (cholla) on rangeland. J. Ecol. 79, 1123–1135.
Andow, D.A., Kareiva, P.M., Levin, S.A., Okubo, A., 1990. Spread of invading organisms. Landsc. Ecol. 4, 177–188.
Ascher, U.M., Greif, C., 2011. A First Course in Numerical Methods. SIAM, Philadelphia, PA, USA.
Casella, G., Berger, R.L., 2001. Statistical Inference. Duxbury press, Pacific Grove, USA.
Dewhirst, S., Lutcher, F., 2009. Dispersal in heterogeneous habitats: thresholds, spatial scales, and approximate rates of spread. Ecology 90, 1338–1345.
Fisher, R.A., 1937. The wave of advance of advantageous genes. Ann. Eugen. 7, 355–369.
Garlick, M.J., Powell, J.A., Hooten, M.B., MacFarlane, L.R., 2013. Homogenization, sex, and differential motility predict spread of chronic wasting disease in mule deer in southern Utah. J. Math. Biol. 69, 369–399.
Garlick, M.J., Powell, J.A., Hooten, M.B., MacFarlane, L.R., 2010. Homogenization of large-scale movement models in ecology. Bull. Math. Biol. 73, 2088–2108.
Hanski, I., Eralahti, C., Kankare, M., Ovaskainen, O., Siren, H., 2004. Variation in migration propensity among individuals maintained by landscape structure. Ecology 7, 958–966.
Haynes, K.J., Cronin, J.T., 2003. Matrix composition affects the spatial ecology of a prairie planthopper. Ecology 84 (11), 2856–2866.
Hengeveld, R., 1988. Mechanisms of biological invasions. J. Biogeogr. 15, 819–828.
Holmes, M.H., 1995. Introduction to Perturbation Methods. Sprinter-Verlag, New York, USA.
Kot, M., Lewis, M.A., Driessche, P.V.D., 1996. Dispersal Data and Spread of Invading Organisms. Ecology 77, 2027–2042.
Kot, M., Neubert, M.G., 2008. Saddle-point approximations, integrodifference equations and invasions. Bull. Math. Biol. 70, 1790–1826.
Moilanen, A., Hanski, I., 1998. Metapopulation dynamics: effects of habitat quality and landscape structure. Ecology 79 (7), 2503–2515.
Morales, J.M., Carlo, T.A., 2006. The effect of plant distribution and frugivore density on the scale and shape of dispersal kernels. Ecology 87, 1489–1496.
Musgrave, J., Lutscher, F., 2014a. Integrodifference equations in patchy landscapes I. dispersal kernels. J. Math. Biol. 69, 583–615.
Musgrave, J., Lutscher, F., 2014b. Integrodifference equations in patchy landscapes II. population level consequences. J. Math. Biol. 69, 617–658.
Neubert, M.G., Kot, M., Lewis, M.A., 1995. Dispersal and pattern formation in a discrete-time predator-prey model. Theor. Popul. Biol. 48, 7–43.
Neupane, R.C., Powell, J.A., 2015. Mathematical model of active seed dispersal by frugivorous birds and migration potential of pinyon and juniper in Utah. Appl. Math. 6, 1506–1523.
Okubo, A., Levin, S.A., 2001. Diffusion and Ecological Problems: Modern Perspectives. Springer-Verlag, New York, Berlin Heidelberg.
Okubo, A., Levin, S.A., 1989. A Theoretical framework for data analysis of wind dispersal of seeds and pollen. Ecology 70, 329–338.
Ovaskainen, O., 2004. Habitat-specific movement parameters estimated using mark-recapture data and diffusion model. Ecology 85 (1), 242–257.
Powell, J.A., Zimmermann, N.E., 2004. Multiscale analysis of active seed dispersal contributes to resolving Reid's paradox. Ecology 85 (2), 490–506.
Raposo, E.P., Bartumeus, F., da Luz, M.G.E., Ribeiro-Neto, P.J., Souza, T.A., Viswanathan, G.M., 2011. How landscape heterogeneity frames optimal diffusivity in searching process. PLoS Comput. Biol. 7 (11), e1002233.
Reeve, J.D., Cronin, J.T., Haynes, K.J., 2008. Diffusion models for animals in complex landscapes: incorporating heterogeneity among substrates, individuals and edge behaviours. J. Anim. Ecol. 77, 898–904.
Robbins, T.C., 2004. Seed Dispersal and Biological Invasion: A Mathematical Analysis (Ph.D. Dissertation). University of Utah, Salt Lake City, Utah.
Shigesada, N., Kawasaki, K., Takeda, Y., 1995. Modeling stratified diffusion in biological invasions. Am. Nat. 146, 229–251.
Skalski, G.T., Gilliam, J.F., 2003. A diffusion-based theory of organism dispersal in heterogeneous populations. Am. Nat. 161, 441–458.
Skellam, J.G., 1951. Random dispersal in theoretical populations. Biometrika 38, 196–218.
Turchin, P., 1998. Quantitative Analysis of Movement: Measuring and Modeling Population Redistribution on Animals and Plants. Sinauer Associates Inc., Sunderland.